Springer

KSME

Journal of Mechanical Science and Technology 31 (2) (2017) 813~821
www.springerlink.com/content/1738-494x(Print)/1976-3824(Online)
DOI 10.1007/s12206-017-0133-1

Multi-response optimization of Nd:YAG laser cutting parameters of Ti-6Al-4V superalloy sheet †

A. Tamilarasan[1,*] and D. Rajamani[2]

[1]*Centre for Advanced Manufacturing and Materials Processing (CAMMP), Department of Mechanical Engineering, Sri Chandrasekharendra Saraswathi Viswa Mahavidyalaya, Kanchipuram-631 561, Tamilnadu, India*
[2]*Centre for Autonomous System Research (CASR), Department of Mechanical Engineering, Veltech Dr. RR and Dr. SR University, Chennai- 600 062, Tamilnadu, India*

(Manuscript Received December 28, 2015; Revised August 8, 2016; Accepted September 16, 2016)

Abstract

This study proposes a multi-response optimization approach for the Nd: YAG laser cutting parameters of titanium superalloy sheet (Ti-6Al-4V). The Box-Behnken design was utilized to plan the experiments, and response surface methodology was employed to develop experimental models. Four input parameters, including pulse width, pulse energy, cutting speed, and gas pressure, were set during the experiment, and kerf deviation and metal removal rate were considered as the performance characteristics. Pores, dross, and striation lines were observed on the kerf wall of the laser-cut surface through scanning electron microscopy. With the suitable mathematical models established, a search optimization procedure based on the use of desirability function was used to optimize the performance characteristics. A confirmation experiment was also conducted to validate the optimized process parameters. The relative error is less than ±2 %, thus confirming the feasibility and effectiveness of the adopted approach.

Keywords: Box-Behnken design; Desirability function; Laser cutting; Optimization; Response surface methodology; Titanium alloy

1. Introduction

Laser cutting is a new advantageous process that breaks through existing cutting technologies. A high potential benefit of laser cutting is currently being applied in automobile, medical instrumentation, and aerospace fields [1]. Laser cutting is a purely non-contact thermal process that transforms electrical energy into high-intensity light energy for flushing materials [2], as illustrated in Fig. 1.

As a result of laser cutting, the different kerf qualities are considered as performance characteristics as depicted in Fig. 2. Alternatively, the present manufacturing scenario is highly advantageous for titanium- and nickel-based superalloys with high complex parts, which include intricate shapes [3]. Among these materials, Ti-6Al-4V alloys are extensively used in aerospace industries because of their inherent superior characteristics, such as high corrosion resistance, high temperature withstanding ability, and low thermal conductivity at elevated temperatures [4]. Ti-6Al-4V alloys exhibit extremely poor machinability because of their high chemical affinity and poor thermal conductivity [5]. Under these circumstances, high-precision laser cutting is an advantageous option for cutting these alloys [6].

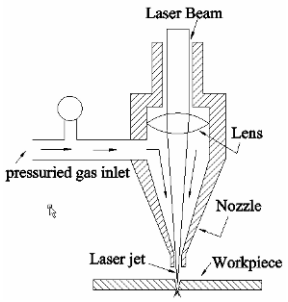

Fig. 1. Schematic of laser cutting.

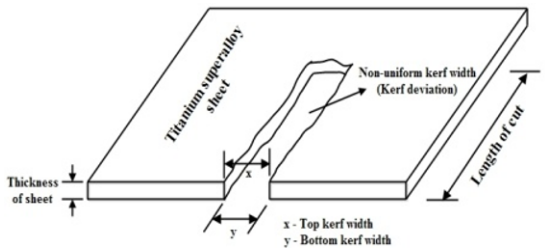

Fig. 2. Kerf qualities of laser cut.

Pulsed Nd:YAG lasers are the best choice for effectively

*Corresponding author. Tel.: +91 9629389136, Fax.: +91 44 27264285
E-mail address: tamilrj2010@gmail.com
† Recommended by Associate Editor Young Whan Park

cutting difficult-to-cut materials because of their greatly improved high beam intensity, fewer Heat-affected zones (HAZs), and narrow-focusing characteristics [7]. However, optimizing the cutting performance of lasers is challenging because of the highly complex input parameters, such as laser energy, pulse width, assist gas pressure, cutting speed, and pulse frequency, in sheet metal cutting [8]. Many studies focused on the various input and output parameters of laser cutting [9-17]. Stournaras et al. [9] experimentally investigated the HAZs, Surface roughness (SR), and Kerf width (KW) in CO_2 laser cutting of aluminum alloy sheet metal and reported that cutting speed and laser power are the significant factors affecting the quality of cut. Ghany et al. [10] cut stainless steel with Nd:YAG laser aiming to achieve a sharp-cut and dross-free surface. Almeida et al. [11] investigated the quality characteristics in Nd:YAG laser cutting of titanium alloy by changing various assisting gases. They reported that inert gases, such as argon and helium, are used to obtain high-quality cuts without any precipitation in cutting edges. Caydas et al. [12] experimentally investigated the SR, kerf taper, and HAZ in Nd:YAG laser cutting of structural 37 steel through grey relational analysis. Yilbas et al. [13] examined the KW in laser cutting of 7050 aluminum alloy reinforced with Al_2O_3 and B_4C composites. The investigation results showed that increasing laser power gradually increases the KW because of the high melting and evaporation on the cutting zone, thereby increasing material removal. Tiwari et al. [14] investigated the influences of process parameters on kerf geometry and HAZ in Nd:YAG laser cutting of nickel-based superalloy. Pandey et al. [15] optimized the Nd:YAG laser cutting parameters, such as SR, kerf taper, and KW, by using grey fuzzy methodology on cutting duralumin sheet with a thickness of 1 mm. Sharma et al. [16] investigated the SR and kerf taper in Nd:YAG laser cutting of nickel-based SUPERNI 718 alloy by using grey relational analysis with entropy measurement. Pandey et al. [17] investigated the quality characteristics in laser cutting of titanium alloy by using genetic algorithm. The group found that cutting speed and pulse frequency are the most significant factors affecting SR and that assist gas pressure and pulse width are the most significant factors affecting kerf taper. Hence, process parameters significantly influence cutting quality. Various optimization approaches have been employed to improve cutting quality characteristics in various engineering materials. Most researchers have focused on optimizing various laser cutting quality characteristics, such as SR, HAZ, and different kerf geometries. However, few studies have attempted to investigate laser cutting performance characteristics, such as Kerf deviation (KD) and MRR. Therefore, the present study aims to optimize laser cutting parameters and consequently enhance performance characteristics for maximum Metal removal rate (MRR) and minimal KD. Experiments were designed using Box-Behnken experimental design considering four process parameters, including pulse width, pulse energy, cutting speed, and gas pressure, with each in three levels.

Table 1. Process parameters and levels.

Process parameter (unit)	Actual symbol	Selected symbol	Coded level		
			−1	0	+1
Pulse width (ms)	X_1	A	1.5	1.75	2
Pulse energy (J)	X_2	B	2.5	4	5.5
Cutting speed (mm/min)	X_3	C	10	14	18
Gas pressure (kg/cm^2)	X_4	D	6	7.5	9

2. Methodologies

2.1 Response surface methodology (RSM)-based box-Behnken design

Myers and Montgomery [18] mentioned that RSM is the sequential method for modeling and optimizing the response variable models involving quantitative independent variables in engineering problems. The Box-Behnken design (BBD) is used in this study as an RSM design because this approach not only can minimize the number of experiments but also evaluate quadratic interactions between pairs of factors. The main selection of BBD should be confined to a situation in which prediction of extreme responses is not of interest. In the present study, pulse width, pulse energy, cutting speed, and gas pressure were selected as process parameters and designated as X_1, X_2, X_3 and X_4, respectively. The low, middle, and high levels of each variable were labeled as −1, 0 and +1, respectively, as shown in Table 1. The variables were coded by the following equation:

$$x_i = \frac{X_i - X_0}{\Delta X} \; i = 1,2,3 \tag{1}$$

where x_i is a dimensionless coded value of X_i, X_0 is the actual value of X_i at the center point, and ΔX is the step change of variable. Five replicates at the center of the design were used to allow the estimation of a pure error sum of squares. The mathematical models of the experimental data provide the second-order polynomial equation for the optimization of the process parameters. The following quadratic (second order) polynomial model explains the behavior of the system:

$$y = \beta_0 + \sum_{i=1}^{k} \beta_i x_i + \sum_{i=1}^{k} \beta_{ii} x_i^2 + \sum_i \sum_j \beta_{ij} x_i x_j + \varepsilon \tag{2}$$

where y is the response and x_i is the value of the i^{th} laser cutting parameters; β_0 is the model constant; β_i represents the linear coefficient; β_{ii} denotes the quadratic coefficient; β_{ij} is the interaction coefficient; k is the number of the process parameters or variables; and ε is the statistical experimental error. The data required for building empirical models are generally collected from experimental design, followed by multiple regression. ANOVA is adopted to justify the significance of the empirical model.

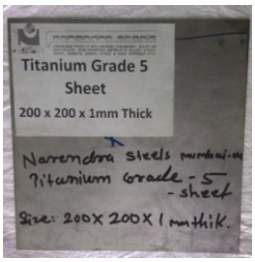

Fig. 3. Ti-6Al-4V superalloy sheet.

2.2 Desirability approach

When several responses were evaluated in an experimental design, the optimum points reached individually for each process parameter did not coincide in all cases [18]. The present study is considered as a multi-response problem to optimize the process parameters simultaneously by using the desirability function approach proposed by Derringer and Suich [19]. This technique is easy and efficient for finding the best range of design space for performance. This approach is used to convert multiple response values into a single dimensionless measure called the overall desirability function. For the scheme of optimization goal within the range, the overall desirability *D* is defined by the equation

$$D = (d_1 \cdot d_2 \cdots d_m)^{1/m}, \tag{3}$$

where *m* is the number of responses in the measure. For each goal, a weight can be assigned to adjust the shape of the particular desirability function. Furthermore, the importance of responses can be varied from zero (least desirable) to five (most desirable). In numerical optimization, the goals are combined to provide the overall desirability function. In general, the obtained overall desirability *D* values lie between 0 and 1. A value of 1 represents the ideal case, and a value of 0 indicates that the responses or process parameters fall outside the desirability range.

3. Experimentation and observations

In the present work, experiments were planned using the BBD of RSM to obtain a quadratic model consisting of 29 trials, including five-center points. The sampled Ti-6Al-4V (grade 5) superalloy sheet with a thickness of 1 mm is depicted in Fig. 3. These alloys are advantageous options and increasingly utilized in high temperature applications because of their excellent heat transfer properties [20].

A series of experiments was performed on a high-precision 300 W pulsed Nd:YAG laser (JK300D model) with a maximum peak power of 16 kW supplied by JK Lasers, UK. An experimental setup along with measurement systems is shown in Fig. 4. Laser parameters nozzle diameter (1 mm), focal length of lens (50 mm), pulse frequency (10 Hz), and cutting length (15 mm) were kept constant throughout the experiment.

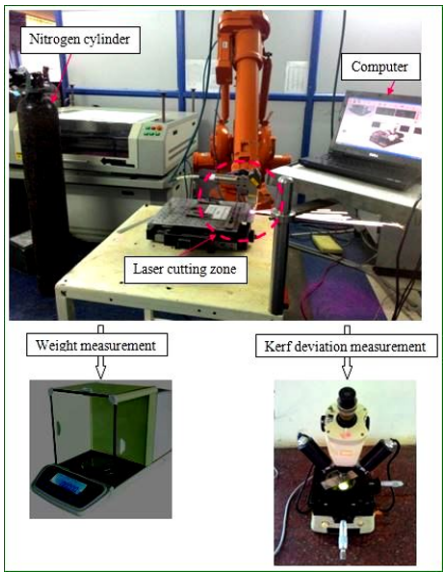

Fig. 4. Experimental setup with measurement systems.

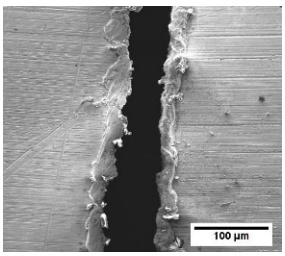

Fig. 5. SEM Result of the 16th trail laser cut.

Nitrogen, which was used as assist gas [21], was injected through a conical nozzle to blow out the melted material and protect the lens from the back-spatter of the molten metal of the workpiece. The top KWs were measured at three locations along the length of the cut. Each experiment was carried out thrice, and their average value was obtained to manipulate the performance characteristics and eliminate statistical errors. KW values were measured using a Vision plus tool maker microscope (Model: METZ-1395, Metzer optical Instruments, India) with a magnification of 30×. Moreover, the result of the 16th experimental trial of the laser cut surface was observed via Scanning electron microscopy (SEM) and is shown in Fig. 5. The KD is the difference between the maximum and minimum top KWs along the cutting length was considered. Mathematically, the KD can be written as

$$\begin{aligned} &Kerf\ \ Deviation,\ KD(mm) \\ &= (Max.top\ \ kerf\ \ width - Min.top\ \ kerf\ \ width). \end{aligned} \tag{4}$$

The weight loss method was used to obtain MRR by weighing the specimen before and after the cutting using Contech electronic balance (Model CAS 234). In addition, the following empirical formula was used to calculate the MRR:

Table 2. BBD layout and results.

Run	A	B	C	D	Kerf deviation	MRR
	ms	J	mm/min	kg/cm^2	mm	mg/min
1	2.00	4.0	18	7.5	0.0146	160.93
2	2.00	4.0	14	6.0	0.0155	88.29
3	1.75	5.5	10	7.5	0.013	166.38
4	1.75	2.5	10	7.5	0.0139	132.33
5	1.75	4.0	14	7.5	0.0123	161.38
6	1.75	5.5	14	9.0	0.0141	56.29
7	2.00	5.5	14	7.5	0.0142	168.19
8	1.75	4.0	18	6.0	0.0121	155.48
9	1.75	4.0	14	7.5	0.0127	160.02
10	1.50	4.0	14	6.0	0.0168	84.89
11	2.00	4.0	14	9.0	0.0144	66.73
12	1.75	4.0	14	7.5	0.0123	174.55
13	1.75	5.5	18	7.5	0.0129	164.33
14	1.50	4.0	14	9.0	0.0197	28.37
15	1.75	4.0	10	9.0	0.0131	156.62
16	1.50	2.5	14	7.5	0.0185	66.05
17	1.75	4.0	10	6.0	0.0145	110.54
18	1.50	4.0	18	7.5	0.0125	74.68
19	1.75	4.0	14	7.5	0.0129	165.92
20	1.75	4.0	14	7.5	0.0126	171.37
21	1.75	4.0	18	9.0	0.0145	66.73
22	2.00	2.5	14	7.5	0.0149	66.73
23	2.00	4.0	10	7.5	0.0101	161.38
24	1.75	2.5	18	7.5	0.0133	123.48
25	1.50	5.5	14	7.5	0.0175	57.20
26	1.75	2.5	14	9.0	0.0187	43.81
27	1.75	2.5	14	6.0	0.0147	77.17
28	1.50	4.0	10	7.5	0.018	147.76
29	1.75	5.5	14	6.0	0.0167	141.41

$$\text{Metal removal rate, } (\text{MRR})(\text{mg/min}) = \left(\frac{\text{Loss of mass during each cut} \times \text{cutting speed}}{\text{Length of each cut}}\right). \quad (5)$$

The measured values of KD and MRR in each experimental run are shown in Table 2.

4. Results and discussion

4.1 Statistical analysis and development of models

Statistical Design Expert v7.0 software was used to evaluate the effects of process parameters, data analysis, and quadratic model building. On the basis of the model described in Eq. (2), the ANOVA details at the 95 % significance level for KD and MRR are depicted in Tables 3 and 4, respectively. Furthermore, the sufficiency of the models was determined using R^2 values, lack-of-fit tests, and model analysis [18]. In general,

Table 3. ANOVA table for KD.

Source	SS	df	MS	*F* value	Prob > *F*
Model	0.0001495	14	1.068E−05	198.647	< 0.0001
A	3.104E−05	1	3.104E−05	577.248	< 0.0001
B	2.613E−06	1	2.613E−06	48.598	< 0.0001
C	6.075E−07	1	6.075E−07	11.297	0.0047
D	1.47E−06	1	1.47E−06	27.336	0.0001
AB	2.25E−08	1	2.25E−08	0.4184	0.5282
AC	0.000025	1	0.000025	464.910	< 0.0001
AD	0.000004	1	0.000004	74.385	< 0.0001
BC	6.25E−08	1	6.25E−08	1.1622	0.2992
BD	1.089E−05	1	1.089E−05	202.514	< 0.0001
CD	3.61E-06	1	3.61E−06	67.133	< 0.0001
A^2	2.95E-05	1	2.95E−05	548.55	< 0.0001
B^2	1.65E-05	1	1.65E−05	306.87	< 0.0001
C^2	5.167E-06	1	5.167E-06	96.084	< 0.0001
D^2	2.329E−05	1	2.329E−05	433.16	< 0.0001
Residual	7.528E−07	14	5.377E−08		
Lack of fit	4.808E−07	10	4.808E−08	0.7071	0.7017
Pure error	2.72E−07	4	6.8E−08		
Cor total	0.0001503	28			
Std. dev.	0.0002319		R^2	0.994	
Mean	0.0145172		Adj R^2	0.989	
C.V. %	1.5973545		Pred R^2	0.978	
Press	3.195E−06		AP	57.737	

Table 4. ANOVA table for MRR.

Source	SS	df	MS	F value	Prob > F
Model	62340.66	14	4452.9045	29.246	< 0.0001
A	5347.09	1	5347.0901	35.118	< 0.0001
B	4970.66	1	4970.6554	32.646	< 0.0001
C	1394.89	1	1394.8864	9.161	0.0091
D	4769.47	1	4769.4723	31.325	< 0.0001
AB	3042.17	1	3042.166	19.980	0.0005
AC	1318.90	1	1318.8953	8.662	0.0107
AD	305.46	1	305.45822	2.006	0.1785
BC	11.59	1	11.591853	0.076	0.7866
BD	669.55	1	669.54545	4.397	0.0546
CD	4544.47	1	4544.4702	29.847	< 0.0001
A^2	12460.76	1	12460.757	81.839	< 0.0001
B^2	6771.65	1	6771.6549	44.475	< 0.0001
C^2	988.96	1	988.95761	6.495	0.0232
D^2	20116.48	1	20116.481	132.121	< 0.0001
Residual	2131.62	14	152.25856		
Lack of fit	1974.75	10	197.47538	5.036	0.0666
Pure error	156.87	4	39.216528		
Cor total	64472.28	28			
Std. dev.	12.34		R^2	0.966	
Mean	117.21		Adj R^2	0.933	
C.V. %	10.53		Pred R^2	0.819	
Press	11619.69		AP	17.891	

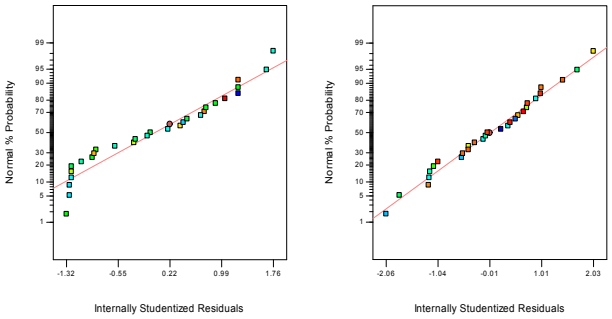

Fig. 6. Normal probability plot for KD and MRR.

the p value was used as a tool to check the significance of the interactions between variables. Statistical significance was considered at $p < 0.05$. Two interaction term coefficients (AB and BC) in Table 3 and three interaction coefficients (AD, BC, and BD) in Table 4 were not significant, and the other term coefficients were significant. Tables 3 and 4 demonstrate that the calculated F and p values are 198.647 and < 0.0001 for KD and 29.246 and < 0.0001, respectively. These F and p values imply that the selected models are highly significant and that the chance that these large *F*-values could be due to noise is less than 0.01 %.

Moreover, Tables 3 and 4 show that the R^2 values for KD and MRR are 0.994 and 0.966, respectively, indicating a high agreement between the experimental and predicted values. The Adj.R^2 value (0.989 for KD and 0.933 for MRR) is similarly high, indicating a high correlation between the observed and the predicted values. The deviations between Adj.R^2 and Pre.R^2 are 0.017 and 0.147 for KD and MRR, respectively, which are lower than the criterion value of 0.2. The lack of fit p values of 0.7071 in KD and 0.0666 in MRR imply that the lack of fit is not significant relative to pure error. The insignificant lack of fit is good because a sufficiently good model fitting is preferred. The adequacy index of the model and adequate precision indicate the accuracy level in application of the test data in building a model, and a value that exceeds 4 more markedly is preferred. In addition to adequacy precision tests, the normal probability plot for KD and MRR is presented in Fig. 6. The figure reveals that the residuals fall on a straight line, implying that the errors are distributed normally and present no obvious pattern and unusual structure, supporting that the terms mentioned in the developed models are significant. From the above analysis and after eliminating the non-significant terms, the final model equations (i.e., in terms of actual values) for KD and MRR are given as follows:

$$\text{KD } (y_1)\text{ (mm)} = +0.19725 - 0.14085A - 0.0004822B - 0.0040568C - 0.007016D + 0.0025AC - 0.002666AD - 0.0007333BD + 0.0001583CD + 0.03412A^2 + 0.0007088B^2 - 0.00005578C^2 + 0.0008422D^2 \quad (6)$$

$$\text{MRR } (y_2)\text{ (mg/min)} = -3146.55204 + 1990.512A - 0.2471B - 13.94C + 436.6D + 73.541AB + 18.158AC - 5.617CD - 701.27351A^2 - 14.360B^2 + 0.7717C^2 - 24.75D^2 \quad (7)$$

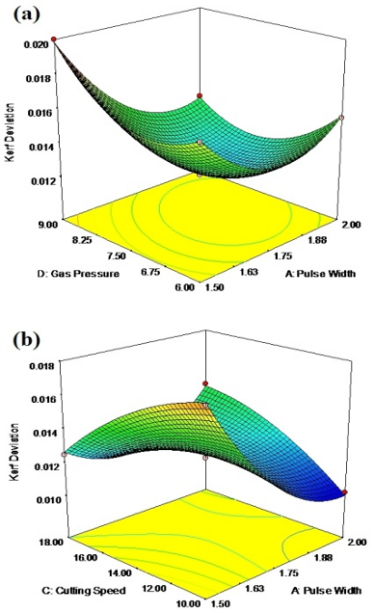

Fig. 7. 3D surface graph for kerf deviation: (a) Pulse width vs. gas pressure; (b) pulse width vs. cutting speed.

where A, B, C and D are the pulse width, pulse energy, cutting speed, and gas pressure, respectively. Overall, statistical analysis reflects that the experimental values fit well with the predicted values and that the accuracy of the model is adequate for further optimization within the limit of the process parameters considered.

4.2 Effect of process variables on KD

Fig. 7(a) shows the response surface and contour plot for KD in relation to pulse width and gas pressure, with the cutting speed and pulse energy values maintained at the middle level. A high gas pressure and low pulse width increase KD. This scenario may be due to the fact that the lower value of pulse width provides intense energy to melt the sheet metal with sufficient time and at a constant cutting speed [22]. In addition, the corresponding cutting conditions of SEM analysis on the laser cut of kerf wall (side view) reveal striation lines, pores, and dross in the result of melting found in Fig. 8. The minimum KD value is achieved at 1.88 ms pulse width and 7.5 kg/cm^2 gas pressure. Fig. 7(b) shows the combined effect of pulse width and cutting speed on KD. KD increases with decreased cutting speed and increased pulse width. Similarly, the SEM image on the kerf wall reflects less surface damage with microstriation lines as observed in Fig. 9.

4.3 Effect of process variables on the MRR

The influence of laser process parameters on the MRR is illustrated in Figs. 10(a) and (b). As shown in Fig. 10(a), the interaction effect of pulse width and pulse energy on the MRR as a bell-shaped response surface is obtained. The maximum

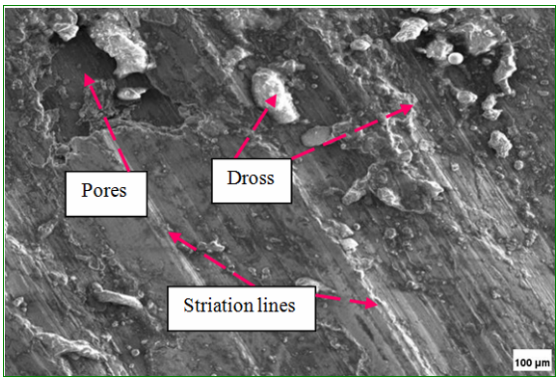

Fig. 8. Kerf wall of laser cut surface.

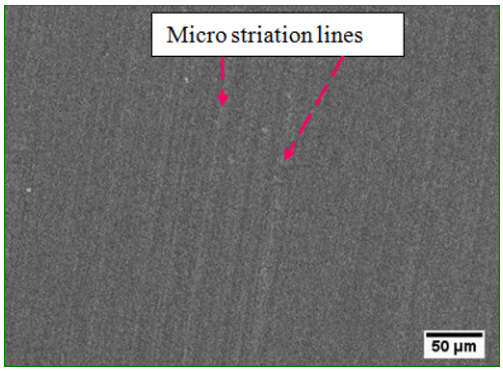

Fig. 9. Kerf wall of laser cut surface.

MRR is recorded in the mid-levels of both process parameters, whereas a further increase in levels gradually decreases the MRR in any direction of pulse width and pulse energy. Fig. 10(b) shows the variation in MRR with pulse width and cutting speed at constant pulse energy (4 J) and gas pressure (7.5 kg/cm^2). Cutting speed is a significant parameter that affects the MRR over pulse width along with the range. Notably, any value of cutting speed along the middle value of 1.75 ms pulse width increases the MRR because the laser beam heat input is totally utilized to melt the workpiece surface in the effect of vaporization temperature [23]. By contrast, the lower value of pulse width results in lower MRR because of lower laser energy hitting the workpiece.

4.4 Multi-response optimization using desirability approach

A single-response optimization algorithm yields a single optimal solution. However, most multi-response problems principally yield a set of optimal solutions instead of a single optimal solution. Ultimately, the multi-response optimization algorithm functions in maintaining a balance between two or more responses in terms of quality and productivity. The present work considers two responses, namely, KD (quality consideration) and MRR (productivity consideration). We observed that KD increases with increasing MRR. Given the production purpose, the optimal combination of parameter levels should produce

Table 5. Design of desirability function.

Name	Goal	Low limit	Up limit	L Wt.	U Wt.	Importance
A	is in range	1.5	2	1	1	3
B		2.5	5.5	1	1	3
C		10	18	1	1	3
D		6	9	1	1	3
KD	min	0.0101	0.0197	1	1	5
MRR	max	28.3723	174.547	1	1	5

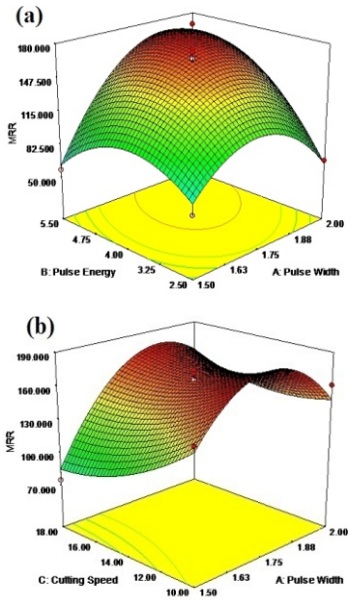

Fig. 10. 3D surface graph for metal removal rate: (a) Pulse width vs. pulse energy; (b) pulse width vs. cutting speed.

the maximum MRR and the minimum KD. The desirability approach is an improved and unique numerical optimization technique used in the industry for the optimization of multiple quality characteristics [19, 24]. The optimization module in Design-Expert searches for a combination of process parameter levels that simultaneously satisfy the requirements placed on each of the responses and process parameters. The developed KD and MRR model equations (3 and 4) were simultaneously solved to yield the optimal process variables. The goal set, lower limits, upper limits, weights used, and importance of the factors given are shown in Table 5.

The minimum and maximum levels were provided for each parameter included. The goals used for kerf deviation and MRR are "minimize" and "maximize", and the goal used for the factors or process parameters is "within range". A weight was assigned to each goal to adjust the shape of its particular desirability function. The importance of each goal was changed in relation to other goals. The default was for all goals to be equally important at a setting of three pluses (+++). Optimization was carried out for a combination of goals. Different best solutions were obtained, and the solution with the

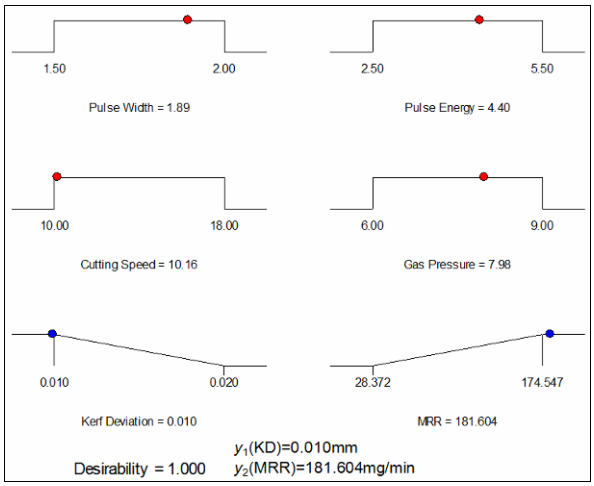

Fig. 11. Desirability ramp for numerical optimization.

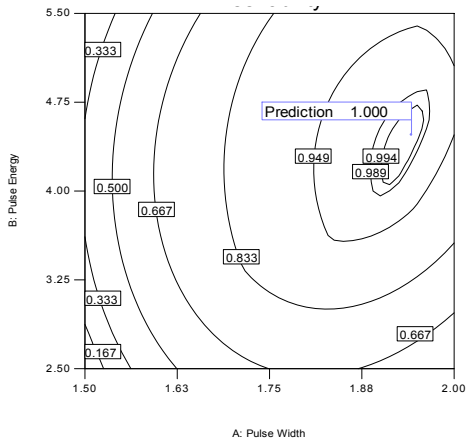

Fig. 12. Estimated contour plot for desirability.

highest desirability is preferred. A linear ramp function was created between lower or higher values to the goal. As illustrated in Fig. 11, the ramp desirability graph reached optimum points through a numerical optimization procedure. The dot of each ramp denotes the reflection of parameter setting, and the amount of desirability is denoted by the height of the dot.

The optimized conditions are 0.010 mm and 181.604 mg/min in the ramp function graph indicated, with the highest desirability value of 1 for KD and MRR under the following optimum process parameters: Pulse width of 1.89 ms, pulse energy of 4.40 J, cutting speed of 10.16 mm/min, and gas pressure of 7.98 kg/cm^2. The contour plots for overall desirability are drawn as shown in Fig. 12 to understand the sensitivity of the results. The optimal region is located at the right-hand side, top part of the graph, which indicates a desirability value of 1.000, which matches the target value.

5. Confirmation experiments

When the optimal levels of the input parameters were selected, the final step was to verify the improvement of laser cut performance by using the optimal levels.

Table 6. Confirmation experiments and their comparison with the results.

Process parameters			
A (ms)	B (J)	C (mm/min)	D (kg/cm^2)
1.89	4.4	10.16	7.98

Responses					
KD (mm)			MRR (m/min)		
Pred.	Actual	Error (%)	Pred.	Actual	Error (%)
0.01	0.0102	1.942	181.604	180.325	-0.7092

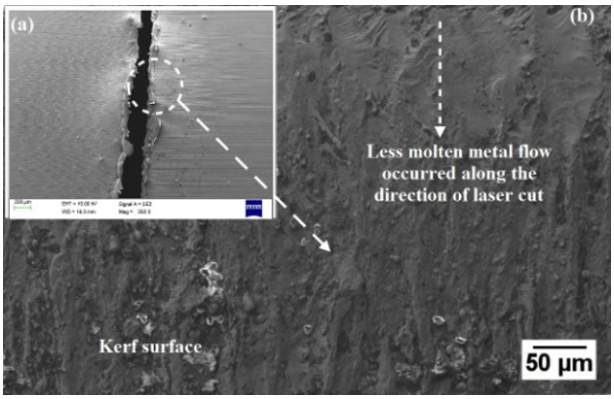

Fig. 13. SEM images on confirmation experiments: (a) Along the length of cut; (b) on the kerf surface.

The experiments were conducted in triplicates, and the average values are reported in Table 6. The confirmation experiment results show that the differences between the predicted and experimental values are less than ±2 %. Hence, this closeness of values confirms excellent reproducibility of the experimental conclusions.

In addition, Figs. 13(a) and (b) are SEM images that correspond to the optimal values of KD and MRR. As shown in Fig. 13(a), small KW variations are observed along the length of the laser cut surface. Moreover, close examination of the kerf surface (i.e., side wall of the laser cut surface) demonstrates the occurrence of a virtually less molten metal flow along the direction of laser cut, as evidently shown in Fig. 13(b).

6. Conclusion

This study optimized the process parameters in Nd:YAG laser cutting of Ti-6Al-4V alloy by using the desirability approach via BBD and RSM. The following conclusions can be drawn from the investigations.

(1) Regression models that relate KD and MRR to the process parameters were developed, and the predicted values match with the experimental values reasonably well, with an R^2 of 0.994 for KD and an R^2 of 0.966 for MRR.

(2) A low cutting speed and a high pulse width produce a

minimal deviation of kerf values.

(3) A low pulse width leads to striation lines, pores, and dross as a result of melting on the kerf surface.

(4) From the multi-response optimization, the optimal parameter settings are as follows: Pulse width of 1.89 ms, pulse energy of 4.40 J, cutting speed of 10.16 mm/min, and gas pressure of 7.98 kg/cm^2. These settings yield high MRR and low KD.

(5) The confirmation experiment results indicate that the predicted values obtained by the mathematical models agree with the actual values.

(6) The confirmation study results show that a dross-free cut can be observed along the kerf edge of the sheet.

(7) This study indicates the application feasibility of the proposed optimization technique for continuous improvement of laser cutting in the manufacturing industry.

References

[1] A. K. Dubey and V. Yadava, Laser beam machining-A review, *International Journal of Machine Tools & Manufacture,* 48 (6) (2008) 609-628.

[2] A. Sharma, Intelligent modelling and multi- objective optimisation of laser beam cutting of nickel based superalloy sheet, *International Journal of Manufacturing, Materials, and Mechanical Engineering,* 3 (2) (2013) 1-16.

[3] A. K. Dubey and V. Yadava, Experimental study of Nd: YAG laser beam machining - An overview, *Journal of Materials Processing Technology,* 195 (1-3) (2008) 15-26.

[4] R. R. Boyer, An overview on the use of titanium in the aerospace industry, *Material Science and Engineering- A,* 213 (1-2) (1996) 103-114.

[5] D. A. Dornfeld, J. S. Kim, H. Dechow, J. Hewson and L. J. Chen, Drilling burr formation in titanium alloy Ti-6Al-4V, *CIRP Annals - Manufacturing Technology,* 48 (1) (1999) 73-76.

[6] A. K. Pandey and A. K. Dubey, Fuzzy expert system for prediction of kerf qualities in pulsed laser cutting of titanium alloy sheet, *Machining Science and Technology: An International Journal,* 17 (4) (2013) 545-574.

[7] G. Kibria, B. Doloi and B. Bhattacharya, Modelling and optimization of Nd:YAG laser micro-turning process during machining of aluminium oxide (Al_2O_3) ceramics using response surface methodology and artificial neural network, *Manufacturing Review*, 1 (2014) 7-14.

[8] F. O. Olsen, Investigations in optimizing the laser cutting process, *International Conference proceedings - American Society for Metals,* Los Angeles (1983) 64-80.

[9] A. Stournaras and P. Stavropoulos, An investigation of quality in CO_2 laser cutting of aluminium, *CIRP Journal of Manufacturing Science and Technology,* 2 (1) (2009) 61-69.

[10] K. Abdel Ghany and M. Newishy, Cutting of 1.2 mm thick austenitic stainless steel sheet using pulsed and CW Nd: YAG laser, *Journal of Materials Processing Technology,* 168 (3) (2005) 438-447.

[11] I. A. Almeida and W. de Rossi, Optimisation of titanium cutting by factorial analysis of the pulsed Nd-YAG laser parameters, *Journal of Materials Processing Technology,* 179 (1-3) (2006) 105-110.

[12] U. Caydas and A. Hascalik, Use of grey relational analysis to determine optimum laser cutting parameters with multi-performance characteristics, *Optics and Laser Technology,* 40 (7) (2008) 987-994.

[13] B. S. Yilbas and S. Khan, Laser cutting of 7050 Al reinforced with Al_2O_3 and B_4C composites, *International Journal of Advanced Manufacturing Technology,* 50 (1) (2010) 185-193.

[14] G. Tiwari and J. K. Sarin Sundar, Influence of process parameters during pulsed Nd: YAG laser cutting of nickel-base superalloys, *Journal of Materials Processing Technology*, 170 (1-2) (2005) 229-239.

[15] A. K. Pandey and A. K. Dubey, Multiple quality optimization in laser cutting of difficult-to-laser-cut material using grey-fuzzy methodology, *International Journal of Advanced Manufacturing Technology,* 65 (1) (2013) 421-431.

[16] A. Sharma and V. Yadava, Optimization of cut quality characteristics during Nd:YAG straight cutting of Ni-based superalloy thin sheet using grey relational analysis with entropy measurement, *Materials and Manufacturing Processes,* 26 (12) (2011) 1522-1529.

[17] A. K. Pandey and A. K. Dubey, Modeling and optimization of kerf taper and surface roughness in laser cutting of titanium alloy sheet, *Journal of Mechanical Science and Technology,* 27 (7) (2013) 2115-2124.

[18] R. H. Myers and D. C. Montgomery, *Response Surface Methodology: Process and Product Optimization Using Designed Experiments*, John Wiley & Sons, Inc.: New York (1995).

[19] G. Derringer and R. Suich, Simultaneous optimization of several response variables, *Journal of Quality Technology*, 12 (1980) 214-219.

[20] M. J. Donachie, *Titanium-a technical guide*, ASM International (1988).

[21] A. K. Dubey and V. Yadava, Multi-objective optimization of laser beam cutting process*, Optics and Laser Technology,* 40 (3) (2008) 562-570.

[22] A. Sharma and V. Yadava, Modelling and optimization of cut quality during pulsed Nd:YAG laser cutting thin Al-alloy sheet for straight profile, *Optics and Lasers in Engineering,* 51 (2013) 77-88.

[23] D. Kondayya and A. Gopala Krishna, An integrated evolutionary approach for modelling and optimization of laser beam cutting process, *International Journal of Advanced Manufacturing Technology,* 65 (1) (2013) 259-274.

[24] A. Tamilarasan and K. Marimuthu, Multi-response optimisation of hard milling process parameters based on integrated Box-Behnken design with desirability function approach, *International Journal of Machining and Machinability of Materials,* 15 (3/4) (2014) 300-320.

A. Tamilarasan is currently working as an Assistant Professor in the Department of Mechanical Engineering, Sri Chandrasekharendra Saraswathi Vishwa Mahavidyalaya, Kanchipuram, Tamilnadu, India. He completed Ph.D. in Mechanical Engineering from Anna University Chennai. He published nine research papers in international journals and four in international conferences. His research includes advanced design and manufacturing engineering, AI techniques, and FEA analysis.

D. Rajamani has completed his B.E. in Mechanical Engineering and M.E. in Engineering Design from Anna University Chennai. He is currently working as a Research Fellow in the Department of Mechanical Engineering, Vel Tech Dr. RR and Dr. SR Technical University, Chennai, Tamilnadu, India. He published four research papers in international journals and two in international conferences. His research includes modern machining process, additive Manufacturing, and Optimization Techniques.